Chapter 2

Thin film deposition and characterisation techniques

2.1 Introduction

The fabrications of electronic components especially solid-state devices, microelectronic integrated circuits and electronic displays have undoubtedly found the widest and most demanding applications for thin film depositions. The functionality of thin films is strongly influenced by their composition and microstructure which can be changed on a large scale depending on the deposition process and the corresponding parameter set-up. Exact knowledge of this interaction is one of the main conditions for setting the thin film functionality needed. Virtually every property of the thin film depends on and can be modified by the deposition process. Microstructure, surface morphology, electrical and optical properties of the thin films are all controlled by the deposition process. A single material can be used in several different applications and technologies and the optimum properties for each application may depend on the deposition technique used. Since not all deposition technologies yield the same properties or microstructures, the deposition process must be chosen to fit the required properties and application.

Basically, thin-film deposition technologies are either purely physical, such as evaporative methods or purely chemical such as gas and liquid-phase chemical processes. A considerable number of processes that are based on glow discharges and reactive sputtering combine both physical and chemical reactions. Physical deposition techniques often result in good quality thin films but the necessity of vacuum, high energy and high quality target make them economically not viable. Further buffer layers synthesized by physical techniques are reported to exhibit comparatively poor photovoltaic conversion

efficiency [1,2]. Unlike the physical methods of preparation of thin films which involve evaporation or ejection of material from a source, chemical methods of thin film deposition entail a definite chemical reaction. In comparison, chemical deposition techniques are less sophisticated and are most suitable for large area deposition. Cost effectiveness of chemical techniques and their feasibility to synthesise variety of materials on different substrates has increased the research interest in these techniques for depositing semiconducting thin films. Eventually chemical deposition techniques have proven to be efficient techniques in synthesizing good quality semiconducting chalcogenide thin films suitable for photovoltaic and optoelectronic applications [3-7].

Among the chemical deposition techniques, liquid phase techniques are more suitable for large area deposition. Hence in the present study the liquid phase chemical deposition techniques, viz. chemical bath deposition (CBD), successive ionic layer adsorption and reaction (SILAR) and photochemical deposition (PCD) have been adopted for synthesizing ZnS/ZnSe thin films for photovoltaic and luminescent applications. These wet chemical synthesis routes do not require vacuum, high temperature or high quality substrates for deposition. The details of the wet chemical synthesis routes adopted in this work are described in the succeeding sections.

2.2 Wet chemical deposition methods

2.2.1. Chemical bath deposition

Chemical bath deposition (CBD) is a simple technique that produces uniform, adherent and reproducible large area thin films for PV and optoelectronic applications. In chemical bath deposition, a complexing agent is used to bind the metallic ions to avoid the homogeneous precipitation of the corresponding compound. Formation of complex ion is essential to

control the rate of the reaction and to avoid the immediate precipitation of the compound in the solution. The metal complex hydrolyses slowly to generate the positive ions in the solution. The solution containing the metal complex is mixed with the solution which produces the negative ion by hydrolyses. The deposition of the compound occurs when the ionic product exceeds the solubility product of the compound to be deposited.

Either homogeneous or heterogeneous deposition can occur. The homogeneous process is the faster one resulting in the deposition of powdery particles on the substrate due to the bulk precipitation. So, the formation of metal complexes is essential to minimize the homogeneous process. In the heterogeneous process, due to the slow release of ions by the metal complexes, the preferential adsorption of ions will take place leading to uniform nucleation and growth of thin film.

CBD is attractive due to its low-cost, low-temperature operation with minimum environmental impact and the flexibility to use a variety of substrates. Further, it is possible to control the film thickness and composition by varying the pH of solution, temperature of bath, time of deposition and concentration of reagents. The main disadvantage of the chemical bath deposition is the wastage of the material due to the deposition on the walls of the container and precipitation into the solution. Preparation of the films with a definite geometric pattern on the substrate is difficult because perfect masking is not possible.

Owing to its simplicity, CBD has been widely used to deposit high quality intrinsic and doped ZnS/ZnSe films and remains the favourite choice of most researchers [8-11]. The CBD experimental set up used to deposit ZnS and ZnSe thin films in the present work is shown in Fig. 2.1.

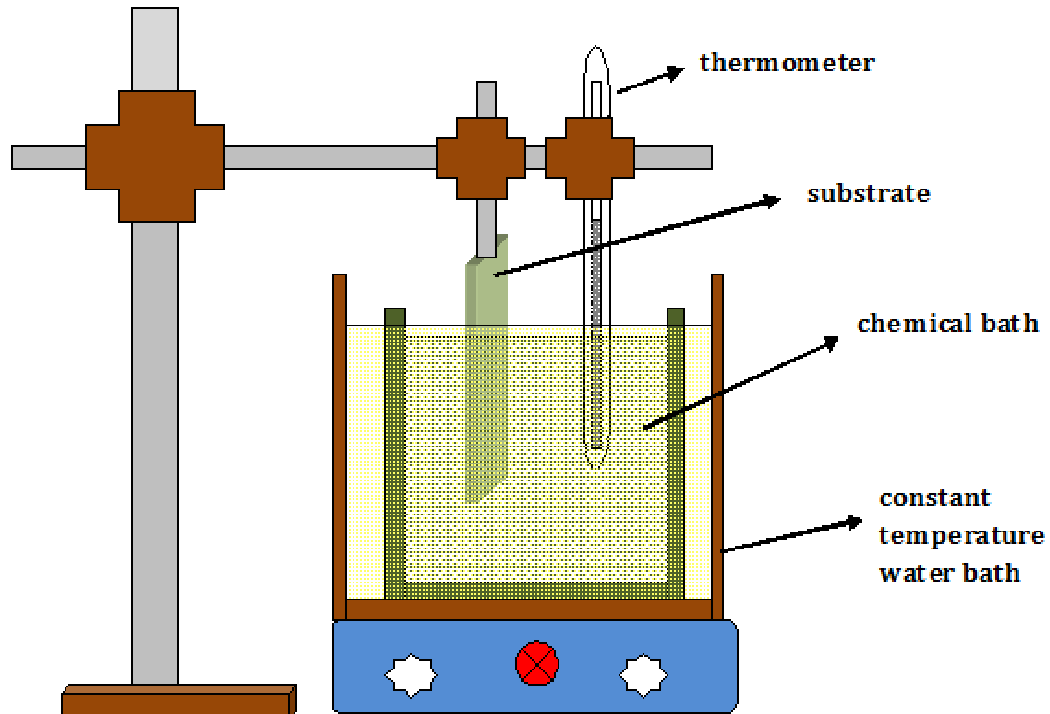

Fig. 2.1: CBD set up

2.2.2 Successive Ionic Layer Adsorption and Reaction

The successive ionic layer adsorption and reaction (SILAR) technique was introduced by Ristov et al. [12] and the name was ascribed by Nicolau [13]. Among the different methods for film deposition, the relative simplicity of SILAR method and its potential application for large area deposition make it very attractive. The SILAR method is based on immersion of the substrate into separate cation and anion precursor solutions, and rinsing in between every immersion with ion-exchanged water to avoid homogeneous precipitation [12-15]. The collection of a substance on the surface of another substance is known as adsorption, which is the fundamental mechanism of the SILAR method. Adsorption is a surface phenomenon between ions and surface of substrate which is possible due to attractive force between them. These forces may be cohesive forces, Vander Waals forces or chemical attractive forces. Atoms or molecules of substrate surface possess unbalanced or residual

force and hold the substrate particles. Sequential reaction at the substrate surface followed by rinsing after each stage enables heterogeneous reaction between the solid phase and the solvated ions in the solution. This method is also known as solution-based atomic layer deposition (SALD) or modified chemical bath deposition (M-CBD). Easy control on film thickness by adjusting number of deposition cycles is the beauty of this method. In principle it is possible to fabricate thin films layer by layer by the SILAR method. Due to the low deposition temperature, diffusion of ions in the thin film is low; hence SILAR is suitable for growing thin multilayered structures. In this method, concentration and of pH cationic and anionic solution, the duration of adsorption, reaction and rinsing are easily controllable.

This environmentally benign soft chemical route has been used to synthesise zinc chalcogenide thin films [16-18] with good optical properties. But SILAR hasn't been much explored to synthesise doped zinc chalcogenide thin films. The microprocessor controlled SILAR deposition set up used in this work is shown in Fig.2.2. In this study SILAR method has been used to deposit pure and doped ZnS thin films and undoped ZnSe thin films. A typical SILAR deposition cycle was comprised of four steps. In the first step the substrate was immersed in the cationic precursor solution for a definite time so that the zinc-complex ions are adsorbed on the substrate. In the next step the substrate was rinsed in distilled water for a definite time to remove the loosely held ions. This is followed by dipping of the substrate in the anionic precursor solution with the chalcogenising agent (thiourea or sodium selenosulphate) during which reaction between cations and anions occurs at the surface of the substrate leading to the formation of ZnS/ZnSe. Finally the

excess unreacted species at the substrate surface was removed by the rinsing in distilled water for the same duration as in the second step.

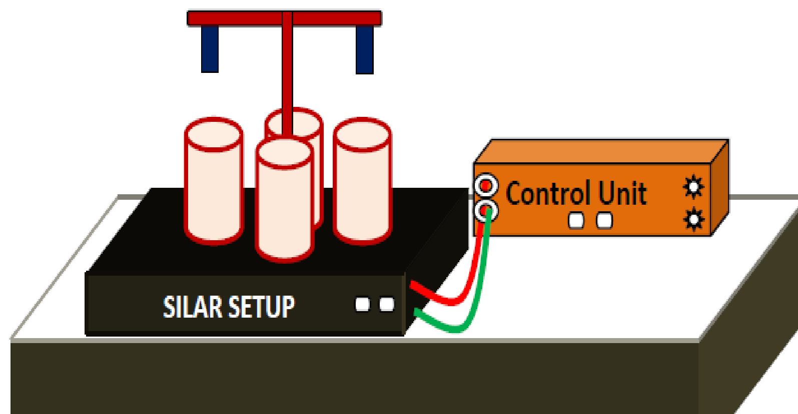

Fig.2.2: SILAR set up

2.2.3 Photochemical Deposition

Photochemical deposition (PCD) technique is a novel technique developed to synthesise compound semiconducting thin films [19-21]. This is a wet chemical route where in the chemical reaction is initiated and film deposition takes place with UV irradiation. This method has the advantage that rate of reaction can be easily controlled by controlling the illumination. In this work PCD technique was used to synthesise pure nanocrystalline ZnSe thin films.

The experimental setup of photo chemical deposition is shown in Fig.2.3. UV lamp of 125W emitting radiation of 355nm is used to illuminate the solution and the substrate. The substrate is kept vertically immersed in the deposition solution within the container such that it is close to the UV source. Quartz beaker is used as the container as absorption of UV radiation by quartz is minimal. In PCD, ZnSe is deposited from an aqueous alkaline bath containing a zinc salt and sodium selenosulphate. Upon ultraviolet illumination the SO_3^{2-}

ions present in the solution absorb UV light and get excited. This photo excited ions release electrons which react with the metal (Zn) and semi metal ions (Se) present in the solution resulting in the formation of ZnSe [22].

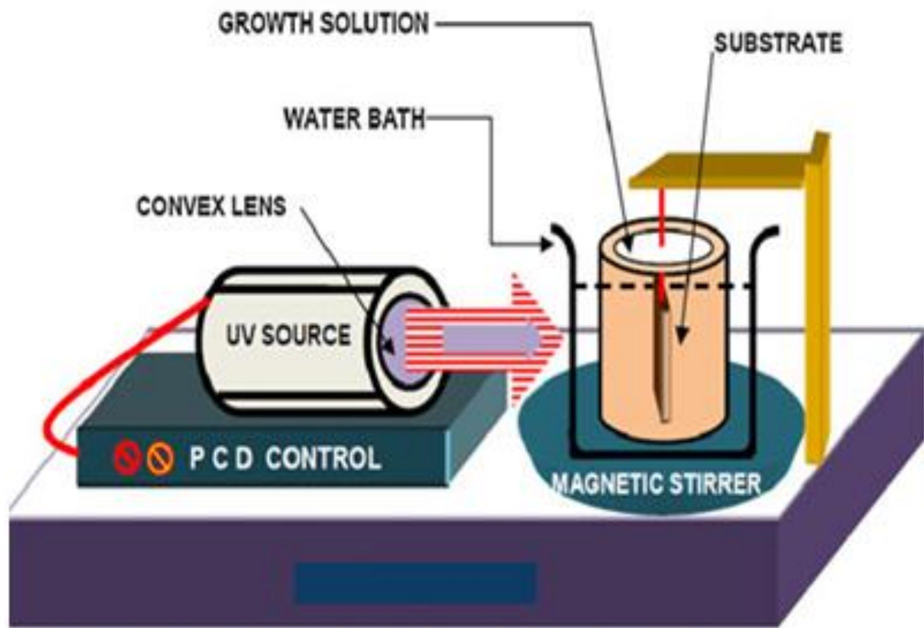

Fig.2.3: PCD set up

2.3 Characterisation tools

The optimization of the preparation conditions is the main task in order to get device quality films. This is to be done on the basis of detailed structural, compositional, morphological, optical and electrical properties of the films obtained at different growth conditions. For a deep understanding of the material properties, characterisation methods for nanostructures should be sensitive to small amount of materials and have high resolution. Various techniques used to characterise ZnS and ZnSe thin films synthesised in the present work are described in the following sections.

2.3.1 Thin film thickness

The effect of film thickness on the properties of thin films is quite instrumental. Reproducible properties are achieved only when the film thickness and deposition parameters are kept invariant. Film thickness may be measured either by in-situ monitoring of the rate of deposition or after the film deposition. In this study two methods were used to estimate the thickness of the film deposited.

(i) Gravimetric method

Gravimetric method [23] of film thickness determination can be adopted if mass of the deposited layer (m), area of deposition (A) and bulk density (ρ) of the material is known. The mass of the deposited film can be determined by estimating the difference in mass between film coated substrate and the bare substrate. The film thickness ‘t’ can be evaluated from the relation,

$$t = \frac{m}{\rho A} \tag{2.1}$$

Here the mass ‘m’ was measured using a high resolution micro balance (Shimadzu AUX 220). The bulk density of ZnS and ZnSe is taken as 4.08 g/cm^3 and 5.27 g/cm^3 respectively.

(ii) Stylus Profiler

The stylus profiler takes measurements electromechanically by moving the sample beneath a diamond tipped stylus. A high precision stage moves the sample according to a user defined scan length, speed and stylus force. The stylus is mechanically coupled to the core of a linear variable differential transformer (LVDT) and moves over the sample surface. Surface variations cause the stylus to be translated vertically. Electrical signals corresponding to the stylus movement are produced as the core position of the LVDT changes. The LVDT scales an ac reference signal proportional to the position change, which

in turn is conditioned and converted to a digital format through a high precision, integrating, analog-to-digital converter [24]. The film whose thickness has to be measured is deposited with a region of the substrate masked which creates a step on the sample surface. The thickness of the sample can be measured accurately by measuring the vertical motion of the stylus over the step. In the present work thickness of the films was measured using Dektak 6M stylus profiler.

2.3.2 Surface morphology

The uniformity and roughness of the thin film surface plays an important role in deciding the optical properties of thin films. When the surface is rough, the films will be less transparent and the grain boundaries will affect the electrical properties of the thin films. The surface morphology of the films was studied using scanning electron microscopy and atomic force microscopy.

(i) Scanning Electron Microscopy

Scanning electron microscopy (SEM) is one of the most widely used techniques for obtaining micro structural and surface features of thin films. SEM has a high resolution and large depth of focus [25,26]. In a SEM a high energy electron beam is focused onto the surface of the specimen and which results in the ionization of the atoms in the specimen. This will cause the ejection of the secondary electrons from the surface, very close to the incident beam position. These secondary electrons can be attracted to a positively charged detector with high efficiency. The secondary electron yield per primary electron is high and increases as the angle between electron beam and the surface normal increases. The secondary electrons generated from the specimens are used for Z-modulation in a corresponding raster on an oscilloscope. In order to avoid charging problems a thin layer of

gold is deposited on the specimen without altering the surface features. The secondary electron mode is generally preferred for topographical feature determination since these electrons generate only from about $10A^0$ or less from the film surface and hence the picture obtained is a faithful reproduction of the surface features. The scanning electron microscopy can be effectively used for the surface analysis to know the details regarding the grain size, presence of minor or secondary phases, the orientation of the grains, uniformity, porosity of the sample etc. In this work the surface morphology of the films was studied using JEOL Model JSM-6490LV electron microscope operated at a voltage of 20kV and probe current of 1nA.

(ii) Atomic Force Microscopy

SEM gives a pictorial overview of the grains on the thin film surface, whereas atomic force microscopy [AFM] is an effective tool to study the surface roughness and also the average cluster size on the thin film surface [27]. AFM can achieve a resolution of 10 pm and unlike electron microscopes, can image samples in air and under liquids.

In AFM a tip integrated to the end of a spring cantilever is brought within the inter-atomic separations of a surface; such that the atoms of the tip and the surface are influenced by inter atomic potentials. As the tip is rastered across the surface, it bounces up and down with the contours of the surface. By measuring the displacement of the tip (*i.e*. the deflection of the cantilever), one can theoretically map out the surface topography with atomic resolution. The AFM is essentially identical in concept to the scanning profilometer, except that the deflection-sensitivity and resolution are improved by several orders of magnitude. The surface topography was investigated using AFM, NT-MDT, Russia (model Ntegra prima) in non-contact mode in the present work.

2.3.3 Compositional analysis

Energy dispersive X-ray analysis (EDAX) was used to estimate the composition of the thin film samples. EDAX analysis system works as an integrated feature of SEM and cannot operate on its own without the latter [28,29]. X rays are generated by the incident electrons within a volume similar to but rather larger than that for the backscattered electrons. Peak X-ray energies corresponding to the characteristics of the elements within that volume can be identified and the relative compositions of elements can be estimated. Thus the bulk composition of the sample and of the individual grains in a polycrystalline sample can be determined. The output of an EDAX analysis is an EDAX spectrum, which is a plot of how frequently an X-ray is received for each energy level. An EDAX spectrum normally displays peaks corresponding to the energy levels for which the most X-rays had been received. Each of these peaks is unique to an atom, and therefore corresponds to a single element. The higher a peak in a spectrum, the more concentrated the element is in the specimen. An EDAX spectrum plot not only identifies the element corresponding to each of its peaks, but the type of X-ray to which it corresponds as well.

In the present work, EDAX measurements were done by the JEOL Model JED-2300 spectrometer operated at a voltage of 20kV and probe current of 1nA which is coupled with SEM.

2.3.4 Structural characterisation

Electrical and optical properties of the materials are influenced by the crystallographic nature of the films. X-ray diffraction (XRD) studies were carried out to study the crystallographic properties of the thin films prepared. A given substance always produces a characteristic X-ray diffraction pattern whether that substance is present in the pure state

or as one constituent of a mixture of substances. This fact is the basis for the diffraction method of chemical analysis. The particular advantage of X-ray diffraction analysis is that it discloses the presence of a substance and not in terms of its constituent chemical elements. Diffraction analysis is useful whenever it is necessary to know the state of chemical combination of the elements involved or the particular phase in which they are present. Compared with ordinary chemical analysis the diffraction method has the advantage that it is much faster, requires only very small sample and is non destructive [29].

The basic law involved in the diffraction method of structural analysis is the Bragg's law. X-ray diffraction methods have very convincingly demonstrated the crystallinity of solids by exploiting the fact that the spacing between atoms is comparable to the wavelength of radiation. This results in easily detected emitted beams of high intensity along certain directions when incident X-rays impinge at critical diffraction angles. Under these conditions the well-known Bragg relation [30],

$$n\lambda = 2d\sin\theta \tag{2.2}$$

holds, where n is the order of diffraction, λ is the wavelength of the X-rays, d is the spacing between consecutive parallel planes and θ is the glancing angle.

X-ray diffraction studies gives a whole range of information about the crystal structure, orientation, average crystalline size and stress in the films[31]. Experimentally obtained diffraction patterns of the sample are compared with the standard Powder Diffraction Files published by the Joint Council of powder Diffraction Standards (JCPDS)

(i) Crystallite size (D)

The average grain size of the film can be calculated using the Scherrer's formula [29, 32],

$$D = 0.94\lambda/\beta cos\theta \tag{2.3}$$

where, λ is the wavelength of the X-ray and β is the full width at half maximum intensity in radians.

(ii) Lattice parameters (a,c)

The lattice parameter values for cubic and hexagonal crystallographic systems associated in the present investigation can be calculated from the following equations using the (h k l) parameters and the interplanar spacing 'd'.

Cubic system,

$$\frac{1}{d^2} = \frac{(h^2 + k^2 + l^2)}{a^2} \tag{2.4}$$

Hexagonal system,

$$\frac{1}{d^2} = \frac{4}{3a^2}(h^2 + hk + k^2) + {l^2}/{c^2} \tag{2.5}$$

(iii) Microstrain (ε)

The presence of strain in the films is inevitable irrespective of the deposition techniques. The strain can be uniform or non-uniform. In the case of uniform strain, the inter-planar lattice spacing 'd' shift to the lower or higher values depending upon the nature of the strain (tensile or compressive) [29,33,34]. Non-uniform strain changes from one region of the grain to another within the same grain. The presence of non-uniform strain is

manifested by the broadening of the X-ray diffraction lines [35]. Information of the strain and the particle size are obtained from the full width at half maximum of the diffraction peaks. The FWHM (β) can be expressed as a linear combination of the contributions from the strain (ε) and crystallite size (D) by the following relation [36],

$$\frac{\beta cos\theta}{\lambda} = \frac{1}{D} + \frac{\varepsilon sin\theta}{\lambda} \quad (2.6)$$

The technique developed by Wiiliamson and Hall (W-H plot) [37] can be utilized to distinguish the effect of crystallite size and strain induced broadening of XRD peaks. W-H plots can be constructed by plotting (βcosθ/λ) against (sinθ/λ). The slope of the plot gives the amount of residual strain. The reciprocal of intercept on (βcosθ/λ) axis gives the particle size.

The microstrain (ε) can be determined using the tangent formula [38],

$$\varepsilon = \frac{\beta}{4tan\theta} \quad (2.7)$$

Microstrain in nanocrystallites in the direction normal to the diffracting plane can also be calculated using the relation [39],

$$\varepsilon = \frac{d_0 - d_s}{d_s} \quad (2.8)$$

where d_s represent the standard value of interplanar spacing of unstressed sample and d_0 represent the observed value of interplanar spacing of stressed sample.

The microstrain in terms of the deviation of lattice parameter a from the bulk value a_0 is given by (40),

$$\varepsilon = \frac{a - a_0}{a_0} \times 100\% \qquad (2.9)$$

The defects in the film can be quantified by computing the dislocation density (δ) by using Williamson-Smallman relation [41],

$$\delta = \frac{1}{D^2} \qquad (2.10)$$

The dislocation density can also be calculated using the alternate formula (42),

$$\delta = \frac{15\beta cos\theta}{4aD} \qquad (2.11)$$

where β is the full width at half maximum, θ is the Bragg's diffraction angle, a is the lattice constant and D is the grain size calculated from XRD pattern.

X-ray diffraction measurements of the films synthesized in this work are done using Bruker AXS-8 advance with Cu-K_α radiation of wavelength 1.5406 A^0 operated at 40 kV and 35 mA.

2.3.5 Optical characterisation

(i) Determination of band gap energy

Intrinsic optical absorption of a single photon across the band gap is the dominant optical absorption process in a solar cell. When the energy of the incident photon (hν) is larger than the band gap energy, the excitation of electrons from the valence band to the empty states of the conduction band occurs. The light passing through the material is then absorbed and the number of electron hole pairs generated depends on the number of incident photons. According to Bardeen et al. [43] for the parabolic band structure, the relation between the absorption coefficient (α) and the band gap (E_g) of the material is given by,

$$\alpha = \frac{A\left(h\nu - E_g\right)^n}{h\nu} \tag{2.12}$$

where, n=1/2 for allowed direct transitions, n=2 for allowed indirect transitions, n=3 for forbidden indirect transitions and n=3/2 for forbidden direct transitions. A is the parameter which depends on the transition probability. The absorption coefficient can be deduced from the absorption or transmission spectra using the relation,

$$I = I_0 e^{-\alpha t} \tag{2.13}$$

where, I is the transmitted intensity, I_0 is the incident intensity of the light and t is the thickness of the film. In the case of direct transition, from eqn. (2.12), $(\alpha h\nu)^2$ will show a linear dependence on the photon energy (hν). A plot of $(\alpha h\nu)^2$ against hν will be a straight line and the intercept on energy axis at $(\alpha h\nu)^2$ equal to zero will give the band gap energy.

(ii) Determination of optical constants

The degree of optical absorption depends on the wavelength of the incident radiation. The optical response of the film in the UV-VIS–NIR region is also affected by properties like refractive index (n), extinction coefficient (k) etc. The refractive index and high frequency dielectric constant (ϵ_∞) of semiconducting materials is very important in determining the electrical properties also. Knowledge of refractive index is essential in the design of hetero structure lasers in optoelectronic devices as well as in solar cell applications.

The extinction coefficient can be determined from the absorption measurements by using the equation [44],

$$k = \frac{\alpha\lambda}{4\pi} \tag{2.14}$$

where α is the absorption coefficient related to the absorbance (A) and thickness (t) of the film by the equation ,

$$\alpha = 2.303A/t \tag{2.15}$$

The refractive index, n can be obtained from the reflectance R and extinction coefficient k using the equation [45],

$$n = \frac{(1+R) + \sqrt{4R - (1-R)^2 k^2}}{(1-R)} \tag{2.16}$$

The refractive index of the films can also be calculated using Moss relation [46, 47] which is directly related to the fundamental energy band gap (E_g),

$$E_g n^4 = k \tag{2.17}$$

where k is a constant with a value of 108 eV. This relation is found to give values in better agreement with the known data for n in II–VI semiconductors [47].

The dielectric behavior of solids is important for several electron-device properties. The spectral data has also been used to obtain the complex dielectric function, of the thin films. The real and imaginary parts of the dielectric function, ϵ and ϵ' are related to n and k by the equations [48],

$$\epsilon = n^2 - k^2 \tag{2.18}$$

$$\epsilon' = 2nk \tag{2.19}$$

The high frequency dielectric constant (ϵ_∞) can be calculated from the following relation [49],

$$\epsilon_\infty = n^2 \tag{2.20}$$

In order to verify the effect of porosity or voids in the films on the refractive index of the layers, the packing density, p, for the films can be calculated using the formula [50],

$$n_f^2 = \frac{(1-p)n_v^2 + (1+p)n_v^2 n_s^2}{(1+p)n_v^2 + (1-p)n_s^2} \tag{2.21}$$

Where n_f is the refractive index of the film at a particular wavelength, n_v is the refractive index of the voids (1 for air) and n_s is the bulk value of refractive index.

2.3.6 Photoluminescence

When an insulator or semiconductor absorbs electromagnetic radiation (i.e. a photon) an electron may be excited to a higher energy quantum state. If the excited electron returns to a lower energy quantum state by radiating a photon, the process is called photoluminescence (PL). The PL intensity depends on the measurement temperature and the energy of the exciting light (known as photoluminescence excitation or PLE spectrum). In general, peaks in the PLE spectrum are higher in energy than those in the PL spectrum. After excitation by an external photon, electron and hole possess high energies due to transitions from their ground state to an excited state. The energies associated with such optical absorptions are directly determined by the electronic structure of the material. The excited electron and hole may form an exciton, as discussed above. The electron may recombine with the hole and relax to a lower energy state, ultimately reaching the ground state. The excess energy resulting from recombination and relaxation may be either radiative (emits photon) or non-radiative (emitting phonons or Auger electrons). Recombination of the electron and hole results in emission of a photon (i.e. radiative recombination leads to PL). Some radiative events from band edge, defects and non-radiative processes are depicted in Fig. 2.4 [51].

(i) Band edge emission

The most common radiative relaxation processes in intrinsic semiconductors and insulators are band edge and near band edge (exciton) emission. The recombination of an excited electron in the conduction band with a hole in the valence band is called band edge emission. An electron and hole may be bound by a few meV to form an exciton. Therefore, radiative recombination of an exciton leads to near band edge emission at energies slightly lower than the band gap.

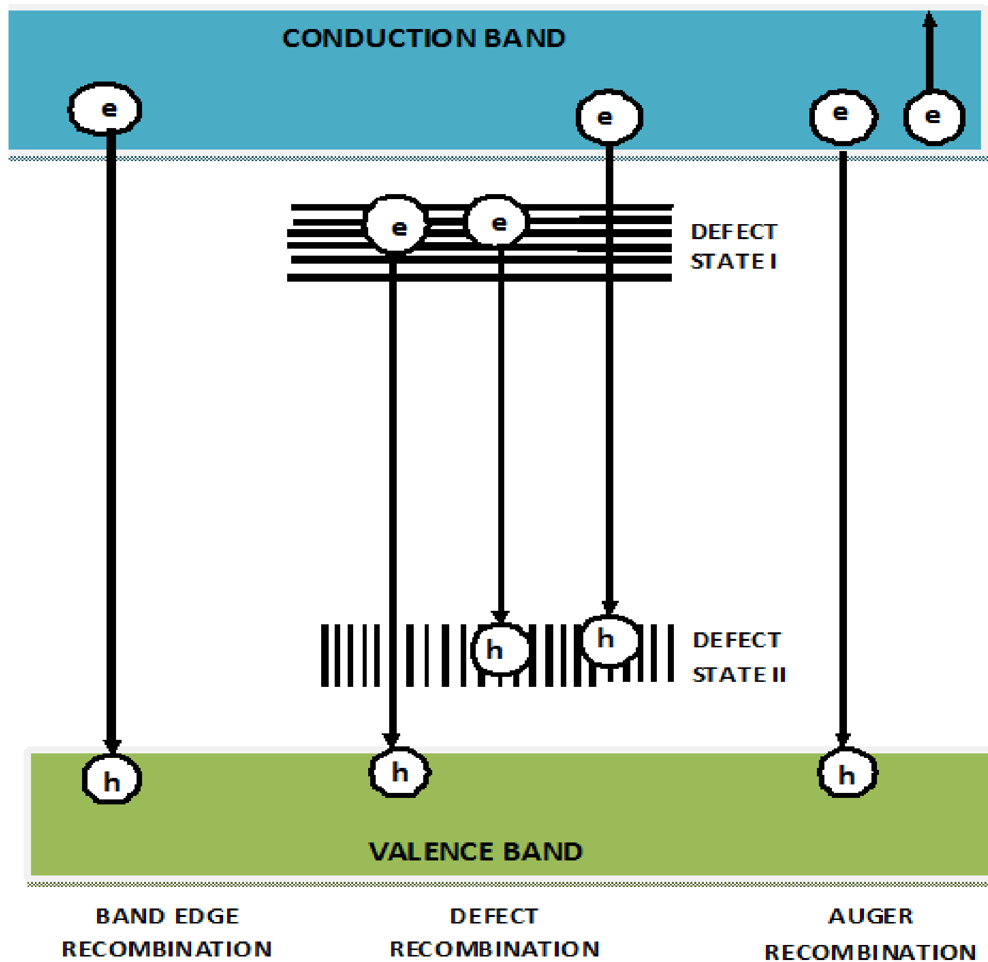

Fig. 2.4: A few radiative and non-radiative processes that can occur during luminescence (e: electron, h:hole)

(ii) Defect emission

Radiative emission from nano phosphors also occurs from localized impurity and/or activator quantum states in the band gap. Defect states are called dark states when they lie inside the bands themselves [52]. Depending on the type of defect or impurity, the state can act as a donor (has excess electrons) or an acceptor (has a deficit of electrons). Electrons or holes are attracted to these sites of deficient or excess local charge due to Coulombic attraction. These defects states can be categorized into either shallow or deep levels, where shallow level defect states have energies near the conduction band or valence band edge. In most cases, a shallow defect exhibits radiative relaxation at temperatures sufficiently low so that thermal energies (kT) do not excite the carriers out of the defects or trap states. Deep levels, on the other hand, are so long-lived that they typically experience non-radiative recombination. Luminescence from these defect levels can be used to identify their energy, and their concentration is proportional to the intensity. Both PL spectral distribution and intensity change with fluctuations in excitation energy due to contributions from different defect energy levels and the band structure of the host.

(iii) Activator emission

Luminescence from intentionally incorporated impurities is called extrinsic luminescence. These impurities are called activators and they perturb the band structure by creating local quantum states that lies within the band gap. The predominant radiative mechanism in extrinsic luminescence is electron-hole recombination, which can occur via transitions from conduction band to acceptor state, donor state to valance band or donor state to acceptor state. In some cases, this mechanism is localized on the activator atom center.

2.3.7. Electrical characterisation

The electrical properties of thin semiconducting films may depend on various factors like deposition method, thickness and homogeneity of the film, crystallinity and grain size, defect concentrations, chemical stoichiometry etc. [48]. The resistivity (ρ) of the films can be calculated applying ohm's law, by the relation

$$\rho = RA/L \tag{2.22}$$

where R is the resistance given by the slope of the current – voltage characteristic curves, A is the area of the film in planar geometry given by the product of the film thickness and the width of the film and L is the spacing between the electrodes.

The resistivity of the films with high resistance was determined by the two-probe method with the electrodes in planar geometry. Highly conducting silver paste was used as the electrodes. The current voltage measurements were carried out using a Keithley`s source measure unit (Model SMU 2400).

The activation energy of charge carriers (E_a) can be determined using the relation

$$\rho = \rho_0 \exp\left(-\frac{E_a}{kT}\right) \tag{2.23}$$

where ρ is the resistivity, k is the Boltzmann constant and T is the temperature. The variation of resistivity of the samples with temperature, in the range 300-480K was studied using the dc four probe method.

References

1. M.M.Islam, S. Ishizuka, A. Yamada, K. Sakurai, S. Niki, K. Sakurai, K. Akimoto, Sol.Energy Mater.Sol.Cells 93(2009) 970
2. D.Abou-Ras, G Kostorz, A Romeo, D Rudmann, Thin Solid Films 480-481(2005)118
3. A. Rumberg, Ch. Sommerhalter, M. Toplak, A. JaÈger-Waldau, M. Ch. Lux-Steiner, Thin Solid Films 361(2000)172
4. D.A. Johnston, M.H. Carlett, K.T.R. Reddy, I. Forbes, R.W. Miles, Thin Solid Films 403–404 (2002)102
5. B.R. Sankapal, S.D. Sartale, C.D. Lokhande, A. Ennaoui, Sol. Energy Mater. Sol. Cells 83(2004) 447
6. P.P. Hankare , P.A. Chate , P.A. Chavan , D.J. Sathe ,J. Alloys Compd. 461(2008)623
7. S.W. Shin, G.L. Agawaneb, M.G. Gang, A.V. Moholkar, J. Moon, J.H. Kim, J.Y. Lee, J. Alloys Compd. 526(2012)25
8. Y. Zhang, X.Y. Dang, J. Jin, T. Yu, B.Z. Li, Q. He, F.Y. Li, Y. Sun Appl. Surf. Sci. 25(2010)6871
9. M. Cao, B.L. Zhang, L. Li, J. Huang, S.R. Zhao, H. Cao, J.C. Jiang, Y. Sun, Y.Shen, Mater. Res. Bull. 48(2013)357
10. C. Hubert, N. Naghavi, B. Canava, A. Etcheberry, D. Lincot, Thin Solid Films 515(2007)6032
11. G.L. Agawane, S.W. Shin, M.P. Suryawanshi, K.V. Gurav, A.V. Moholkar, J.Y. Lee, P.S. Patil, J. H. Yun, J.H. Kim, Mater. Lett. 106(2013)186
12. M. Ristov, G.J. Sinadinovski, I. Gorzdanov , Thin Solid Films 123(1985)63
13. Y.F. Nicolau, Appl. Surf. Sci. 22/23 (1985)1061
14. S. Lindroos, T. Kanniainen and M. Leskela, Appl. Surf. Sci. 75(1994)70.
15. Y.F. Nicolau, M. Dupuy and M. Brunei, J. Electrochem. Sot. 137 (1990) 2915
16. M. AliYildirim , Aytunc- Ates, Aykut Astam, Physica E 41(2009)1365.
17. R.B. Kale, C.D. Lokhande, Mater. Res. Bull. 39(2004)1829.

18. B. Guzeldir, M. Saglam, A. Ates, J. Alloys Compd. 506(2010)388.
19. F.Goto,M.Ichimura, E.Arai, Jpn.J.Appl.Phys. 36(1997)L1147
20. M.Ichimura, F.Goto,Yuhei Ono,E.Arai, Jour.Crys.Growth.198/199(1999)308
21. M.Ichimura, K.Takeuchi, A. Nakamura, E.Arai, Thin Solid Films, 384(2001)137
22. R.Kumaresan, M.Ichimura, E.Arai, Thin Solid Films 414(2002)25
23. P.S. Patila, R.K. Kawara, T. Sethb, D.P. Amalnerkarb, P.S. Chigare, Ceramics International 29(2003)725
24. P. E. J. Flewitt, R. K. Wild, Physical methods for materials characterisation, IOP Publishing Ltd, 2003
25. K.Oura, V.G Lifshits, A.A Saranin, A.V Zotov, M.Katayama, Surface science an introduction, Springer-Veralg, Heidelberg, Germany 2003.
26. G.I. Goldstein, D.E. Newbury, P.Echlin, D.C Joy, C.Fiori, E.Lifshin, Scanning electron microscopy and x-ray microanalysis, New York: Plenum Press, 1981
27. P. E .J. Flewit, R. K. Wild, Physical methods for material characterisation, IOP publishing, London, 2003
28. D. K. Schroder, Semiconductor material and device characterisation, A Wiley-interscience publication, New York, 1998.
29. B.D. Cullity, S.R. Stock, Elements of X ray diffraction, Prentice Hall, New Jersey, 2001
30. C. Kittel, Introduction to Solid State Physics, Wiley Eastern Limited, New Delhi, 1996
31. C.S. Barrett, Structure of Metals-CrystallographicMethods, Principles and Data,Mcgraw-Hill Book Company,New York, 1943
32. Bob B. He, Two-dimensional X-ray diffraction, John Wiley&Sons,Inc., Hoboken, New Jersey, 2009
33. C.R. Fell, M. Chi., Y.S. Meng, J.L. Jones, Solid State Ionics 207(2012)44
34. C.Krill, R.Birringer, Philos.Mag.A 77(1998)621

35. J. Mazher, A.K. Srivastav, R.V. Nandedkar, R.K. Pandey, Nanotechnology 15 (2004) 572.
36. S.B. Quadri, E.F. Skelton, D. Hsu, A.D. Dinsmore, J. Yang, H.F. Gray, B.R. Ratna, Phys.Rev. B 60 (1999)9191.
37. K.Williamson, W.H. Hall, Acta Metall. 1(1953)22
38. H.P.Klug, L.E. Alexander, X-ray diffraction procedures for polycrystalline and amorphous materials, Wiley, NewYork, 1974
39. E. Sinha, S.K Rout, Bull.Mater.Sci. 32(2009)65
40. N. Choudhury, B.K. Sarma, Indian J. Pure Appl. Phys. 46(2008) 261
41. X.S Wang, Z.C Wu, J.F Webb, Z.G Liu, Appl.PhyS. A 77 (2004)561
42. Y.P. Venkata Subbaiah, P. Prathap, K.T. Ramakrishna Reddy, Appl. Surf. Sci. 253 (2006) 2409
43. J.Bardeen, F.J.Blatt and L.H. Hall, Proceedings of Photoconductivity Conf, Atlantic City, 1954
44. R. Swanepoel, J.Phys.E:Sci.Instrum.16(1983) 1214
45. F.Gode, Physica B 406 (2011)1653
46. L. Hannachi and N. Bouarissa, Physica B 404 (2009) 3650
47. V. P. Gupta and N. M. Ravindra, Phys. Status Solidi B 100 (1980)715
48. A.Goswami, Thin Film Fundamentals, New Age International(P) Limited, New Delhi,1996
49. E. H. Rhoderick, R.H. Williams, Metal-Semiconductor Contacts, Clarendon Press, Oxford,1988
50. M. Harris, H.A. Macleod, S.Ogura ,Thin Solid Films 57(1979)173
51. A. Kitai, Luminescent Materials and Applications , John Wiley & Sons Ltd., England, 2008
52. A. Issac, C .von Borczyskowski, F. Cichos, Phys. Rev. 71(2005)16.